

DIVINER LUNAR RADIOMETER EXPERIMENT EXTENDED MISSION RESULTS: THERMAL, THERMOPHYSICAL, AND COMPOSITIONAL PROPERTIES. D. A. Paige¹, B. T. Greenhagen², and the Diviner Science Team; ¹Dept. of Earth and Space Sciences, University of California, Los Angeles, CA, USA. Email: dap@moon.ucla.edu; ²Jet Propulsion Laboratory, California Institute of Technology, Pasadena, CA, USA

Introduction: The Diviner Lunar Radiometer is the first infrared instrument to globally map the thermal emission from the moon's surface and its diurnal and seasonal variability. After over three and a half years in operation, analysis of Diviner's unprecedented dataset has revealed the extreme nature of the Moon's thermal environment, its thermophysical properties, and surface composition. This presentation will highlight contributions from many members of the Diviner Science Team addressing a diverse range of scientific questions.

Diviner Lunar Radiometer: The Diviner Lunar Radiometer is a nine-channel, pushbroom mapping radiometer that has operated nearly continuously onboard the Lunar Reconnaissance Orbiter since July, 2009. Diviner measures broadband reflected solar radiation with two channels, and emitted thermal infrared radiation with seven infrared channels [1]. The two solar channels, which both span 0.3 to 3 μm , are used to characterize the photometric properties of the lunar surface. The three shortest wavelength thermal infrared channels near 8 μm were specifically designed to characterize the mid-infrared "Christiansen Feature" emissivity maximum, which is sensitive to silicate composition [2]. Diviner's longer wavelength thermal infrared channels span the mid- to far-infrared between 13 and 400 μm and are used to characterize the lunar thermal environment and thermophysical properties [3,4].

Diviner has now acquired observations over six complete diurnal cycles and three complete seasonal cycles. Diviner daytime and nighttime observations (12 hour time bins) have essentially global coverage, and more than 75% of the surface has been measured with at least 6 different local times. During the LRO circular mapping orbit, Diviner's spatial resolution was ~200m. During the LRO elliptical extended mission orbit, Diviner's resolution is varying between 150 m to 1300 m. Calibrated Diviner data and global maps of visible brightness temperature, bolometric temperature, rock abundance, nighttime soil temperature, and silicate mineralogy are available through the PDS Geosciences Node [5,6].

Thermal Environment: The lunar thermal environment is complex and extreme. Surface tempera-

tures in equatorial regions such as the Apollo landing sites are close to 400K at noon and less than 100K at night, with annual average temperatures at depth of approximately 250K (Figure 1) [7]. Diviner has mapped the poles at diurnal and seasonal temperature extremes and the data show that large areas within permanently shadowed craters have annual maximum temperatures approaching 50K (Figure 2) [3]. The coldest multiply-shadowed polar craters have temperatures low enough to put constraints on lunar heat flow [8]. Diviner data have also been used to estimate the thermal properties of non-polar permanently shadowed regions [9].

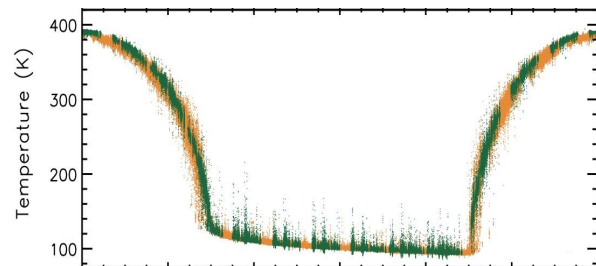


Figure 1: Diviner Equatorial Temperature Curve. The green data represent maria (darker, more rocky) and the orange data represent highlands (lighter, less rocky).

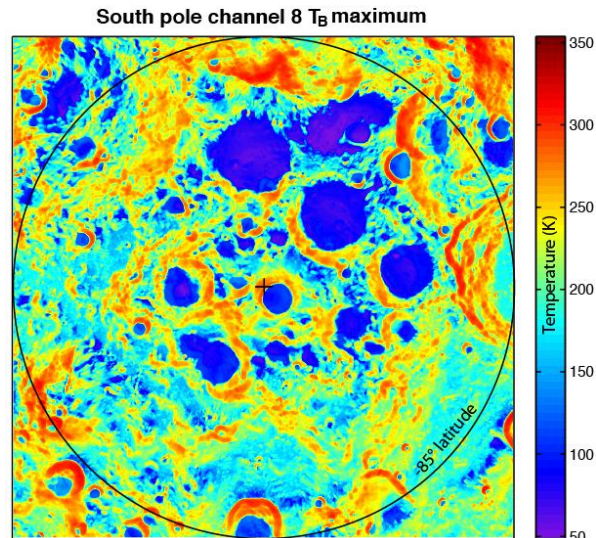


Figure 2: South Pole Annual Maximum Temperatures. The extreme low temperatures observed at the lunar poles are cold enough to trap a wide range of volatile species.

Thermophysical Properties: Diviner is directly sensitive to the thermophysical properties of the lunar surface face including nighttime soil temperature, rock

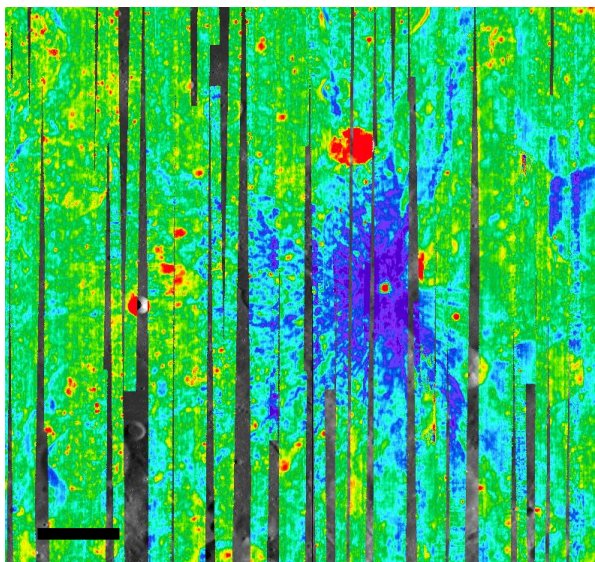


Figure 3: Equatorial Cold Spot at 90.8°E, 5.4°S. The extended blue area surrounding the small crater in the center of this map is ~10 degrees colder than typical regolith. (Scale bar is 25 km)

abundance, and surface roughness. Although much of the Moon has uniform regolith thermal properties, some fresh impact craters cool to lower than normal temperatures. Hundreds of these “cold spots” (Figure 3) have been observed distributed across all lunar terrain types and may indicate a lower-density surface layer [4]. By modeling the higher thermal inertia of rocks, which stay warmer than lunar soil at night we have demonstrated the ability to quantify the areal rock fraction (Figure 4) [4]. Diviner is also sensitive to roughness.

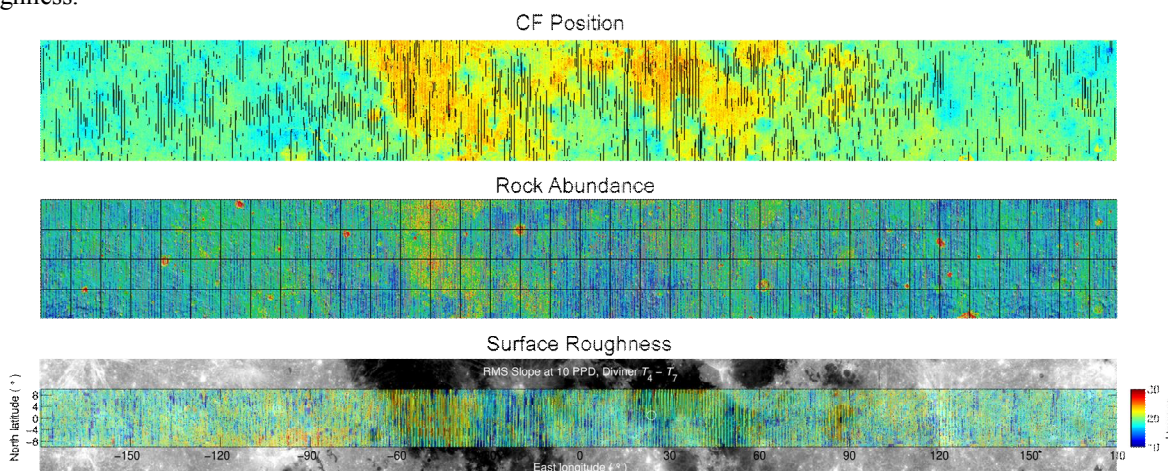


Figure 4: Comparison of Diviner-derived equatorial properties (-15° to +15°N). Top: Diviner silicate composition with blues more feldspathic and reds more mafic. Middle: Diviner rock abundance with reds rockier. Bottom: Surface roughness with reds rougher.

on the mm scale and the multispectral nature of the dataset has been used to model RMS surface slopes and show that on these scales the maria are generally rougher than the highlands (Figure 4).

Compositional Properties: Diviner was designed to characterize the Christiansen Feature (CF) and constrain lunar silicate mineralogy (Figure 4) [2]. The CF is tied to the fundamental SiO₂ vibrational band and shifts to shorter wavelengths with increasing silicate polymerization. Leveraging the relatively restricted geochemistry of the lunar surface, we have used Diviner observations of Apollo sites, and laboratory measurements of Apollo soils to infer some geochemical abundances (e.g. FeO) [10]. Diviner is sensitive to the presence of high silica minerals such as quartz or alkali feldspar and has been used to localize these minerals on the lunar surface [11,2]. Diviner data also provided an important constraint on plagioclase abundance that can be used to infer the amount of country rock mixing [2] and when combined with near-infrared datasets can reveal more than either dataset individually.

References:

- [1] Paige D.A. *et al.* (2010) *SSR*, 150. [2] Greenhagen B.T. *et al.* (2010) *Science*, 329, 1507. [3] Paige D.A. *et al.* (2010) *Science*, 330, 479. [4] Bandfield J.L. *et al.* (2011) *JGR*, 116. [5] Paige D.A. *et al.* (2011) *LPSC XLII*, #2544. [6] Greenhagen B.T. *et al.* (2011) *LPSC XLII*, #2679. [7] Vasavada A.R. *et al.* (2012) *JGR*, 117. [8] Siegler M.A. *et al.* (2012) *NLSI LSF*. [9] McGovern J.A. *et al.* (2012) *JGR*, submitted. [10] Allen C.C. *et al.* (2012) *JGR*, in press. [11] Glotch T.D. *et al.* (2010) *Science*, 329, 1510.